Fermi National Accelerator Laboratory
FERMILAB-Pub-88/96-A
July 1988

MICROWAVE ANISOTROPY PATTERNS FROM EVOLVING STRING NETWORKS[1]

FRANÇOIS R. BOUCHET,[♡♮◇♣] DAVID P. BENNETT,[♠♯] AND ALBERT STEBBINS[♯]

♠ Astronomy and Astrophysics Center, University of Chicago
♣ Centre de Physique Théorique de l'Ecole Polytechnique, Palaiseau, France
♡ Department of Astronomy, University of California, Berkeley
◇ Institut d'Astrophysique de Paris, France
♮ Institute of Geophysics and Planetary Physics, Lawrence Livermore National Laboratory
♯ NASA/Fermilab Astrophysics Center

ABSTRACT. In this article we present estimates of the cosmic microwave background anisotropy that is produced by a network of cosmic strings. String networks were evolved dynamically in a flat matter-era cosmology[1,2] Using a formalism[3] for calculating microwave anisotropy generated gravitationally by moving objects we have computed the temperature patterns produced by these networks. Inherent inaccuracies of our technique for calculating $\Delta T/T$ are discussed. The angular size of our temperature maps depends on the redshift of last scattering but will be in the range $7° - 40°$. The temperature maps have $(\Delta T/T)_{\rm RMS} \sim 17G\mu/c^2$ where μ is the model-dependent linear mass density of the strings. Comparison with anisotropy experiments places an upper limit of 5×10^{-6} on $G\mu/c^2$. The "stringy," non-Gaussian character of the temperature fields is illustrated.

Presently the only known physical mechanisms for producing the observed cosmological inhomogeneities involve either cosmic strings or quantum fluctuations produced during an inflationary epoch[4] Cosmic strings are linear topological defects that are predicted by some grand unified theories to form during a spontaneous symmetry breaking phase transition in the early universe[5] In inflationary scenarios only the density inhomogeneities and a gravitational wave background survive to be detected during the present epoch, and neither of these would carry any unambiguous signature of their inflationary origin. In contrast, in the string scenarios, the strings themselves survive to the present epoch and have the unique observable signature of producing discontinuous jumps in the intensity of the microwave background radiation (MBR)[6,7]

In order to estimate the sensitivity of anisotropy experiments to the temperature patterns expected from strings requires knowledge of the statistical properties of the string networks. It is expected that these networks evolve toward an equilibrium "scaling solution". Thus the present properties of the network may be determined without knowledge of the initial conditions. Numerical simulations of string networks in an expanding universe have demonstrated the existence of the scaling solution and revealed some of the properties of this equilibrium[1,2] We have taken one such matter era ($a \propto t^{2/3}$) simulation and used the time evolution of the network to estimate the temperature pattern that would be produced by the strings in the simulation if viewed at a distance.

[1]submitted to *NATURE*

This work was supported in part by the NSF (at Berkeley and Chicago), the DOE (at Fermilab and IGPP), and by NASA (at Fermilab).

Geometry of the String Simulation

Here we explain the geometry of the string simulation. For details of numerical technique and a description of the results regarding the strings we refer the reader to refs. 1 and 2. The string simulation was done in a cube of fixed comoving size with periodic boundary conditions. The initial horizon-size ($3t$) was 0.25 times the cube size and the simulation continued for an expansion factor of 16 so that the final horizon size was equal to the cube size. If z_i is the epoch at the start of the simulation then the comoving size of the box is

$$L = \frac{2}{0.25}\frac{c}{H_0}(1+z_i)^{-\frac{1}{2}} = 759\sqrt{\frac{1000}{1+z_i}}\, h_{100}^{-1}\mathrm{Mpc} \qquad (1)$$

The photons for which the temperature shift was calculated consisted of three planes of photons moving in the x, y, and z directions each of which had time to cross 0.75 of the cube length during the run. The geometry is such that these are approximately the photons we would see at a single instant if $z_f = \frac{z_i}{16} \gg 1$. The temperature shifts we have calculated for these photons are only those from the $L \times L \times 0.75L$ subset of our cube which the photons have swept out. These photons will subtend a square on our sky with angular size

$$\theta_L = \frac{\Theta_{H_i}}{0.25} \qquad \Theta_{H_i} = \frac{1}{\sqrt{z_i}}\ \mathrm{rad.} = 1.8^\circ\sqrt{\frac{1000}{1+z_i}} \qquad z_i \gg 1, \qquad (2)$$

where Θ_{H_i} is the apparent angular size of the horizon at z_i. In the matter era the projected angular length of string in the redshift interval $[z_i, z_f]$ scales as

$$\theta_{\mathrm{string}} \propto \sqrt{z_i} - \sqrt{z_f} \qquad z_f \gg 1 \qquad (3)$$

for a random patch of sky where we have assumed $\Omega_0 \approx 1$. Thus most of the visible strings are concentrated at high redshifts near the surface of last scattering. In this letter we shall take the simulation volume to be up against the surface of last scattering, i.e. $z_i = z_{ls}$. We are thus missing no visible strings from in back of the simulation cube, but we are missing strings from between the cube and us. Equation (3) tells us that we have included only 75% of the string that should be included for $z_{ls} \approx 1000$ (which is correct if the universe was not reionized soon after recombination). To compensate for this we have placed two simulation volumes end to end and thus cover an expansion factor of 256. The photons we are considering start traversing the second simulation volume when $1+z$ is 16 times less than when they started traversing the first simulation volume. Equation (2) then tells us that the comoving size of the second simulation volume, L', must be 4 times larger that of the first, L. Hence we only need consider $\frac{1}{16}$ of the photons traversing the second volume. The composite map now includes all but 6% of the correct number of strings for $z_{ls} \approx 1000$. On the other hand, if the universe becomes reionized at high redshifts then then z_{ls} could be as low as 30. In this case we have included about 18% too many strings. We feel this is a good compromise given the uncertainties of reionization. The redshift of last scattering also determines the angular size of the region for which we have calculated the temperature pattern as shown by equation (2). Thus the apparent angular size of our temperature pattern should be in the rather large range $\theta_L \in [7^\circ, 40^\circ]$. While observers might wish for firmer predictions, theoretical uncertainties just do not allow it. The ionization history of the universe will depend on the efficiency of primordial star formation which is not well understood.

The Temperature Calculation

The gravitational fields of strings produce significant anisotropies in the microwave background because of their relativistic motions.[6,7] To calculate the temperature pattern from this effect we have used a Fourier version of the flat-space formalism given in ref. 3. With this method we can impose periodic boundary conditions on the temperature pattern to go along with the periodic boundary conditions of the string simulation. This formalism is not generally applicable to an expanding universe. However, as we shall describe, we do not expect the formalism to give too bad an estimate of the anisotropy. A proper cosmological treatment of the anisotropy with present techniques would be much more computer intensive and would thus yield results with a much smaller dynamic range. Furthermore the peculiar stringy nature of the temperature patterns depends on short angular distance behavior of the anisotropy pattern which is accurately represented in our results.

The formalism used gives an accurate estimate of the temperature shift induced by a segment of string for light rays which pass much closer than the horizon distance from the segment but overestimates the effect for light rays with larger impact parameters. Thus our maps should contain spuriously large temperature anisotropy for large angular wavelengths but should be fairly accurate for wavelengths smaller than the projected horizon size. Many of the qualitative features we are interested in here should not be affected by this long wavelength component of the temperature pattern. We shall also see that even with the non-cosmological formalism there is a natural low frequency cutoff at about the projected horizon size due to the coherence length of the strings themselves. Other effects neglected by our technique are

(1) Sachs-Wolfe effect from potential perturbations at the surface of last scattering,

(2) Sachs-Wolfe effect from decaying-mode potential perturbations between the surface of last scattering and us,

(3) Anisotropies from baryonic perturbations at the last scattering surface,

(4) Anisotropies from gravitational waves emitted by strings before last scattering,

(5) Possible secondary anisotropies should the universe become reionized and from foreground sources.

We expect that (2), (3) and (4) should lead to smaller amplitude perturbations than those discussed here, although we have no space to justify these sentiments here. Effect (5) is very model dependent and could be important or negligible. Effect (1) is probably the most important and its amplitude could be comparable to the one we are considering.[8,9] If the universe does not become reionized we would expect that the coherence angle of this component of anisotropy would be fairly small ($\sim 10'$) because the surface of last scattering is fairly thin ($\Delta z_{ls}/z_{ls} \sim 0.1$). However if the universe is reionized then it is likely that $\Delta z_{ls}/z_{ls} \sim 1$ and the surface of last scattering would only contribute to longer wavelength ($\sim \Theta_{H_l}$) anisotropies. While many of the stringy features of the temperature pattern will persist if $\Delta z_{ls}/z_{ls} \sim 1$, detecting these features may be problematic if there is no reionization and $\Delta z_{ls}/z_{ls} \sim 0.1$. In any case the reader should consider these calculations as idealized in such a way as to make their stringy character most evident.

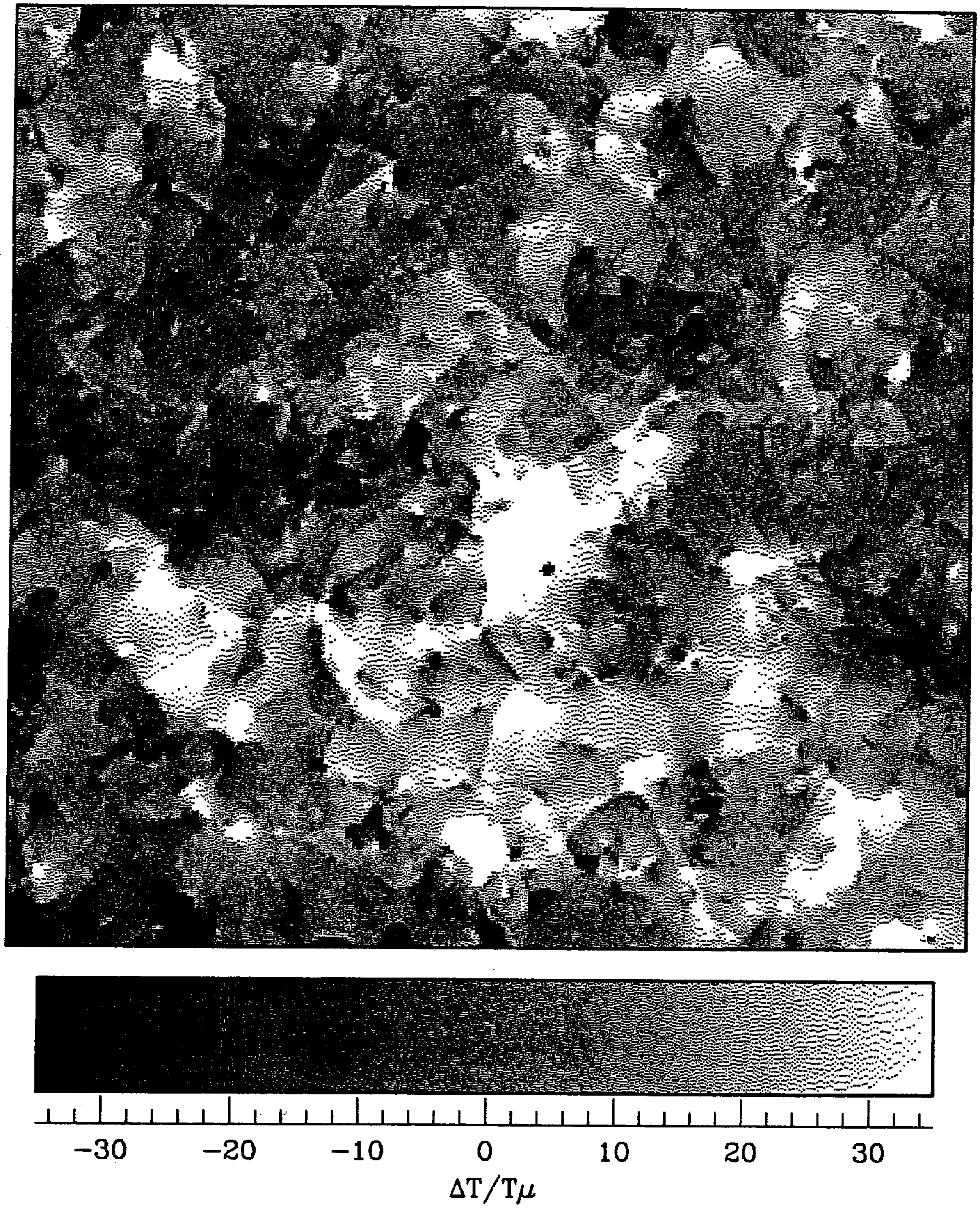

Fig. 1

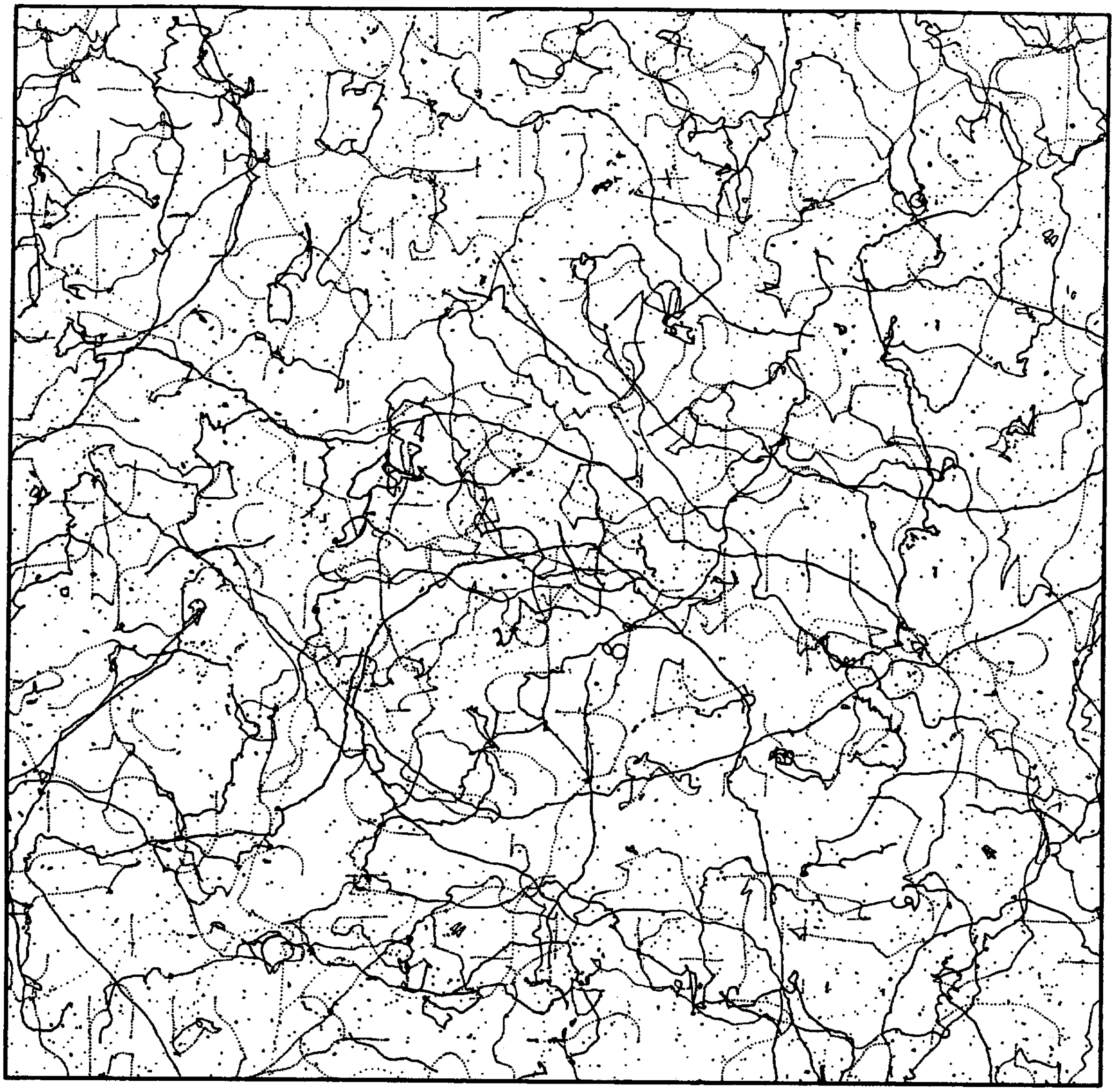

Fig. 2

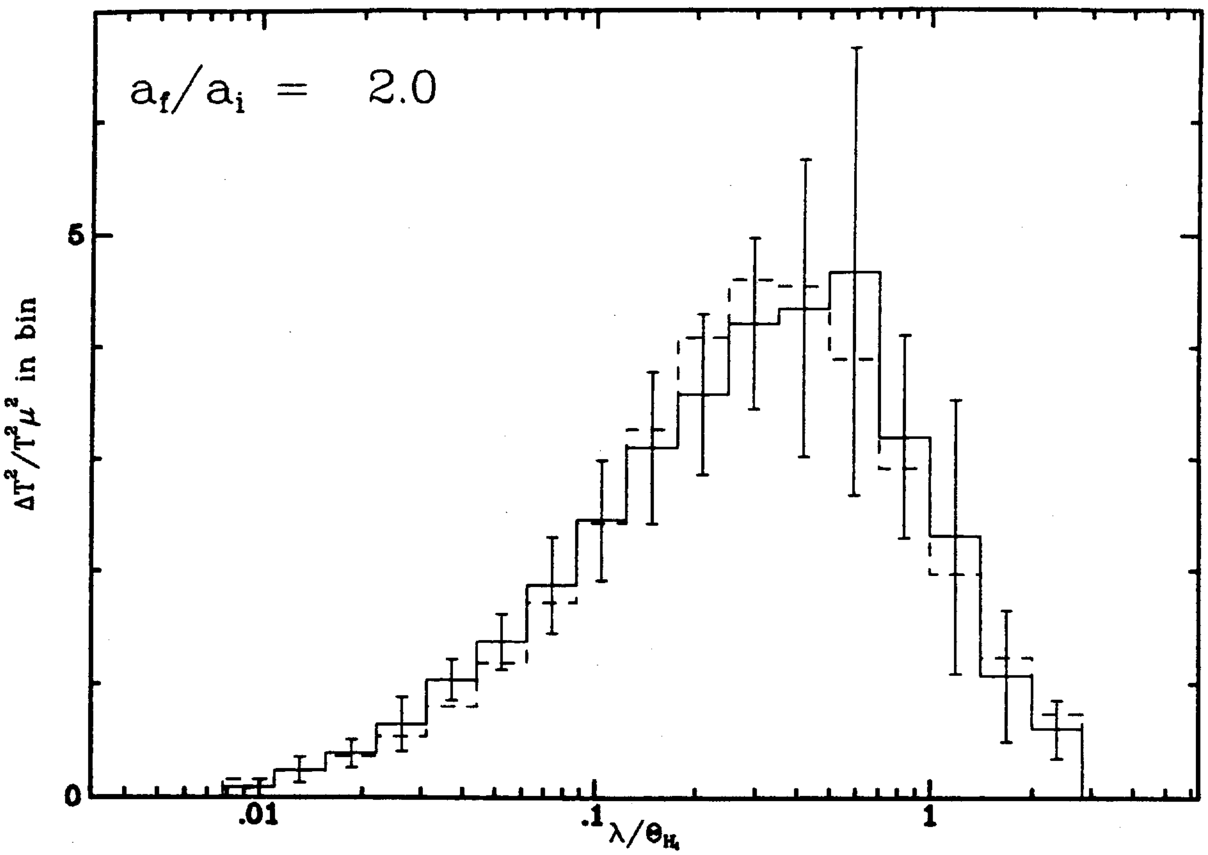

FIGURE 3. The power ($\Delta T^2/T^2 \times (G\mu/c^2)^{-2}$) in various wavelength bins in the anisotropy pattern produced as a string network expands by a factor of 2. Θ_{H_i} refers to the initial angular size of the horizon. The error bars are the standard deviation about the mean for 12 different slices through a single simulation. The dashed line is an analytic fit.

(1,1) modes in the rest of our discussion. Aside from the fundamental modes there is no clearly significant evolution of the power spectra when compared to run to run variations. Undoubtedly this is partially due to the small number of simulations, but in any case we feel that for the purposes of anisotropy the strings are close enough to the scaling solution that this is not a major inaccuracy in our method.

In figure 3 we present the average of as well as the standard deviation of the power in various wavelength bins for all of the 12 slices (4 slices per direction, 3 directions) that we have calculated. There is a clear peak at about half the horizon size which is the imprint of the coherence length of the strings on the temperature pattern they induce. There is also some evidence for convergence at both long and short wavelengths. Cosmological corrections to our formalism should cut off the long wavelengths more sharply, but given the cutoff that is already present it is not clear this will make much of a difference. To make the results displayed in figure 3 more useful we give a fit to this spectra. The total power in wavelengths shorter than a wavelength λ_* is well fit by the function

$$P_2(\lambda < \lambda_*, \Theta_{H_i}) = \frac{\Delta_2 T}{T}^2 \left(\frac{\lambda_*^{1.7}}{(0.6\Theta_{H_i})^{1.7} + \lambda_*^{1.7}}\right)^{0.7} \quad \text{where} \quad \frac{\Delta_2 T}{T} \approx 6\frac{G\mu}{c^2}. \qquad (4)$$

The quantity $\frac{\Delta_2 T}{T}$ is the rms anisotropy from strings in the redshift interval z to $2z$. The

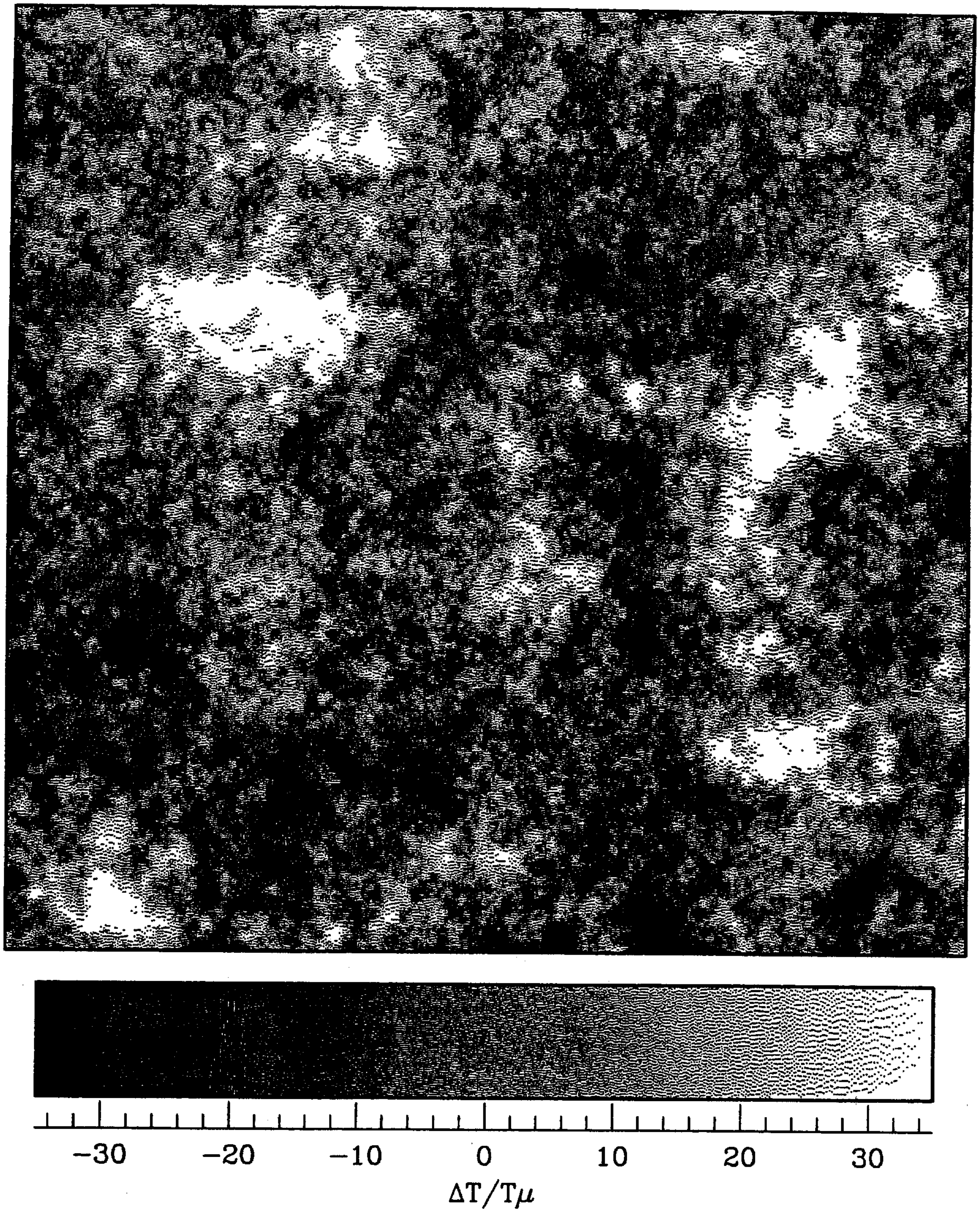

Fig. 4

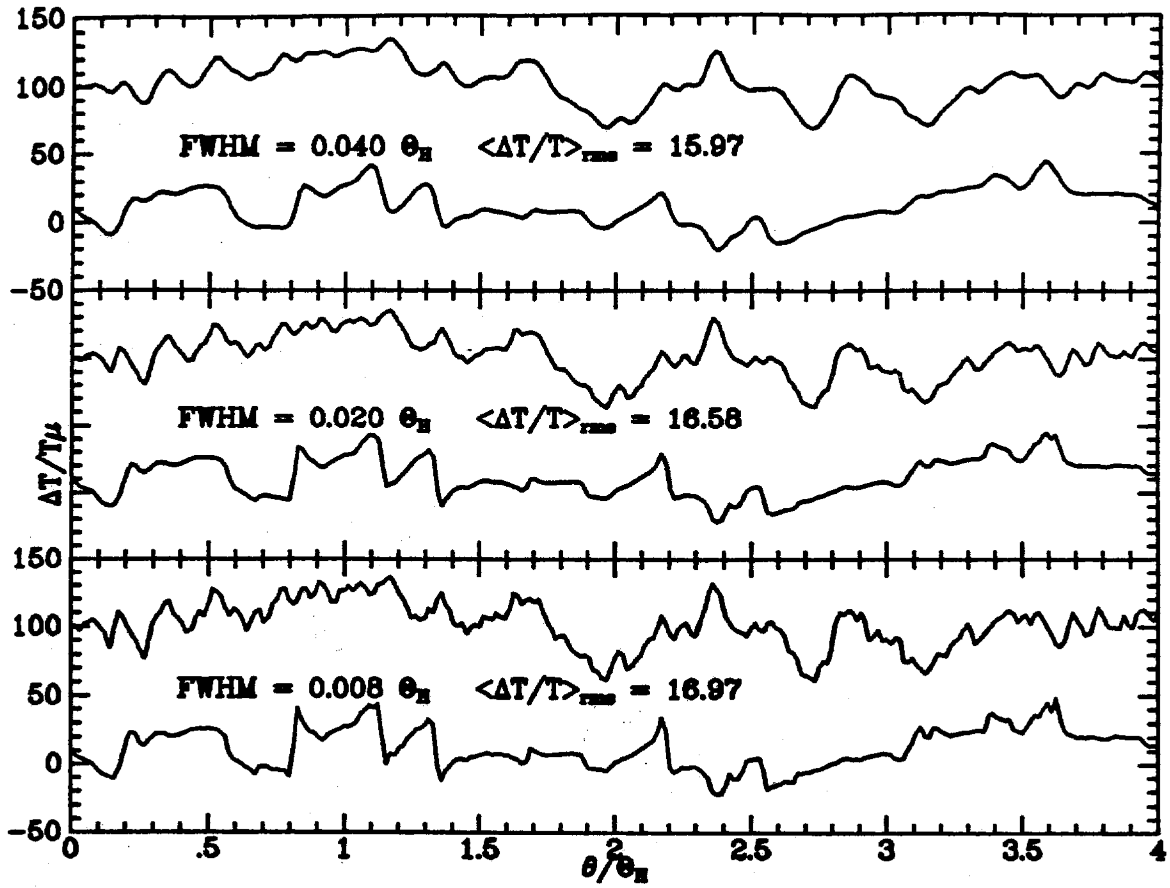

FIGURE 5. **Shown are the responses of three single beam detectors if they were to make a linear scan across the string temperature map (Fig. 1). Displaced 100 units above is a scan through the random phase temperature map (Fig.4). The three detectors have FWHM beamwidths $4'\sqrt{1000/(1+z_{ls})}$ (top curves), $2'\sqrt{1000/(1+z_{ls})}$ (middle curves), and $0.9'\sqrt{1000/(1+z_{ls})}$ (bottom curves). The angular length of each scan is the same as the angular size of the 2-d maps, i.e. $7.2°\sqrt{1000/(1+z_{ls})}$.**

will allow for actual detection of strings. To illustrate the effect of these phase correlations, we have Fourier transformed the temperature maps we had combined to produce figure 1. We then changed the phase of each Fourier amplitude to a random number and combined the two maps in the same way we produced figure 1. The resulting pattern is shown in figure 4. This second image has exactly the same power spectrum, but the phase coherence has been lost. The high frequency modes do not interfere constructively with the low frequency ones to produce sharp features, but give rise to many small scale fluctuations. Another way to see the difference between random Gaussian fluctuations and "stringy" ones is to examine one-dimensional scans of the two temperature maps (figures 1 and 4). Figure 5 shows three such scans for each temperature map. The three pairs of scans differ only in that the temperature patterns have been smoothed (in 2 dimensions) with different Gaussian windows for each scan. The full width at half maximum for these scans are 0.04, 0.02, and 0.008 of Θ_{H_i} or 4, 2, and $0.9 \times \sqrt{1000/z_{ls}}$ arc minutes. It is clear that a FWHM of 2 arc minutes is quite sufficient in order to distinguish the flat plateaus and sharp jumps of the "stringy" temperature pattern from its Gaussian counterpart. For $z_{ls} \approx 1000$ this begins to be somewhat more difficult (though still possible) with a FWHM of 4 arc minutes.

4. R. Brandenberger, *Inflation and Cosmic Strings: Two Mechanisms for Producing Structure in the Universe*, Int. J. Mod. Phys. **A2** (1987), 77.

5. A. Vilenkin, *Cosmic Strings*, Phys. Rev. **D24** (1981), 2082.

6. N. Kaiser and A. Stebbins, *Microwave Anisotropy due to Cosmic Strings*, Nature **310** (1984), 391.

7. R. Gott, *Gravitational Lensing Effects of Vacuum Strings: Exact Solutions*, Astrophys. J. **288** (1985), 422.

8. R. Brandenberger and N. Turok, *Fluctuations from Cosmic Strings and the Microwave Background*, Phys. Rev. **D33** (1986), 2182.

9. J. Traschen, N. Turok, and R. Brandenberger, *Microwave Anisotropy from Cosmic Strings*, Phys. Rev. *D* **34** (1986), 919.

10. F. Melchiorri, B. Melchiorri, C. Ceccarelli, and L. Pietranera,, Astrophys. J. Lett. **250** (1981), L1.

12. C. J. Hogan and M. J. Rees, *Gravitational Interactions of Cosmic Strings*, Nature **311** (1984), 109.

13. R. L. Davis, *Nucleosynthesis Problems for String Models of Galaxy Formation*, Phys. Lett. **161B** (1985), 285.

14. D. P. Bennett, *Evolution of Cosmic Strings II*, Phys. Rev. **D34** (1986), 3592.

15. J. Silk and A. Vilenkin, *Cosmic Strings and Galaxy Formation*, Phys. Rev. Lett. **53** (1984), 1700.

16. N. Turok and R. H. Brandenberger, *Cosmic Strings and the Formation of Galaxies and Clusters of Galaxies*, Phys. Rev. **D33** (1986), 2175.

17. R. Brandenberger, N. Kaiser, D. Schramm, and N. Turok, *Galaxy and Structure Formation with Hot Dark Matter and Cosmic Strings*, Phys. Rev. Lett. **59** (1987), 2371.

18. E. Bertschinger and P. N. Watts, *Galaxy Formation with Cosmic Strings and Massive Neutrinos*, Astrophys. J. **328** (1988), 23.

FRANÇOIS R. BOUCHET **601 Campbell Hall, University of California, Berkeley, CA 94720**
DAVID P. BENNETT **MS 209, Fermilab, Box 500, Batavia, IL 60510**
ALBERT STEBBINS **MS 209, Fermilab, Box 500, Batavia, IL 60510**